

II. Sample Distribution Network

Before starting to explain the optimization method, the sample DN is described in advance. In order to simulate the coordination of the load transfer between feeders and comprehensive operational optimization, a multi-secondary substations (S/S) and multi-feeders DN with high renewable DERs penetration is chosen to be the sample system in this paper, as shown in Fig. 1. The sample system is an 11 kV radial distribution system having two substations, four feeders, 70 buses, and 78 branches (including 11 tie-branches) [10], and 19 switches assumed. The feeders F1 and F2 are fed by S/S-1; and the feeder F3 and F4 are fed by S/S-2. The 11 tie-branches (TSs) tie-1~tie-11 which are normally opened interconnect with these four feeders. The DERs are placed throughout feeders, the type, size, and location of renewable DGs are assumed in this paper, as listed in Table 1

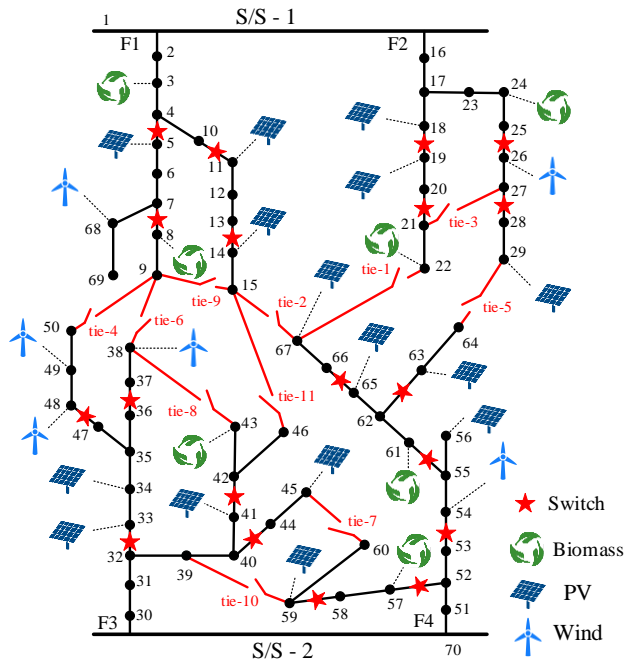


Fig. 1 Single line diagram of the sample DN

Table 1 The rated outputs, types, and locations of the DGs

Feeder	Type	Location Bus	Rated output(kW)
F1	PV	5, 11, 14	125, 25, 75
	Wind	68	50
	biomass	3, 8	25, 50
F2	PV	18, 19, 29	75, 100, 125
	Wind	26	100
	biomass	22, 24	50, 25
F3	PV	33, 34, 41, 45	75, 100, 100, 150
	Wind	38, 48, 49	50, 75, 50
	biomass	43	75
F4	PV	56, 59, 63, 65, 67	150, 25, 100, 150, 100
	Wind	54	100
	biomass	57, 61	50, 50

For the time series based simulation, the dynamic load and DG generation data must be considered. The entire annually patterns of load and renewable DGs generation are used to calculate the yearly sequential power flow, so that

the dynamic MG boundaries can be decided by the solution results. Four types of load pattern are used to the four feeders, which are office, residential, industrial, and commercial, respectively. These four types of weekly load pattern are shown in Fig. 2. In addition, the daily pattern average power output of wind and PV for each month are presented to depict the characteristics of the renewable generation, as shown in Fig. 3. It's clear from this patterns that the PV output is higher in daytime and summer; the wind power output is higher in winter.

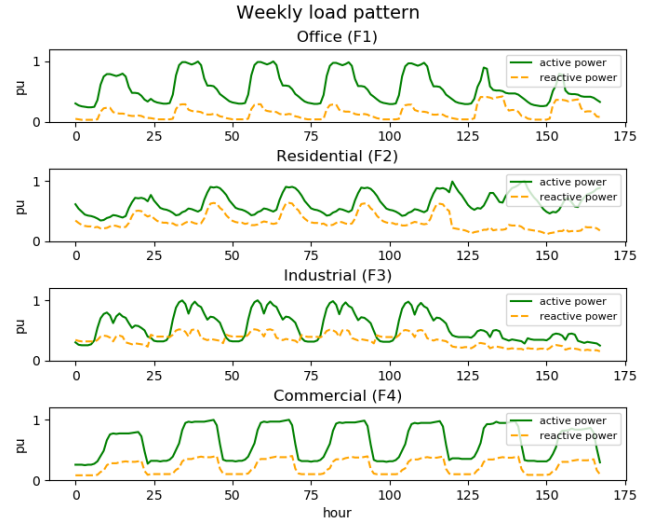


Fig. 2 Weekly load pattern

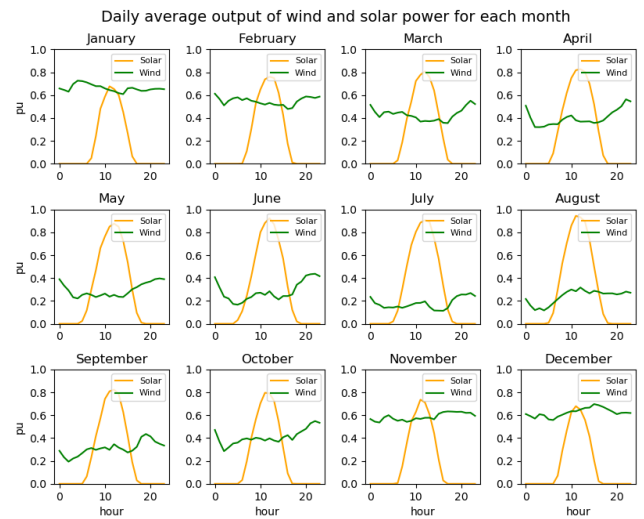


Fig. 3 Daily pattern of power output of wind and PV for each month

III. Optimization Method

3.1 Problem Description

The three-phase unbalance in DNs is caused by the single phase distribution transformers or laterals, symmetrical three-phase distribution transforms with unbalanced loads, and the asymmetrical three-phase distribution transformers like U-V connection and V-V connection. The U-V connection, also known as open-wye and open-delta connection, is a three-phase arrangement that makes use of only two, instead of three, single-phase transformers which is modified from wye-delta connection. Likewise, the V-V connection, also known as open-delta

connection, is modified from delta-delta connection. These asymmetrical connections are sometimes used in distribution transformers for economy and saving space; however, the problems of three-phase unbalance hence exacerbated. The possible connection schemes for the three-, two-, or single-phase transformers and laterals are different. To solve this problem, all the connection of transformers on the feeders must be rearranged to make the loads evenly distributed to each phase. All six types of three-phase transformer connection schemes are shown in Fig. 4, and the optimization algorithm is used to find the best arrangement of all transformers connection varying among these six types for each season.

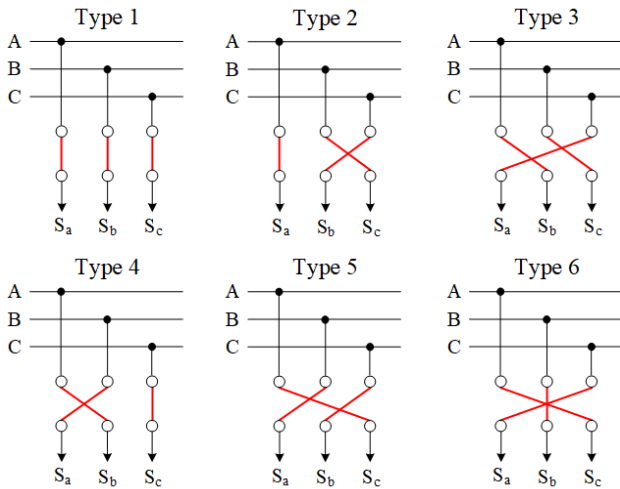


Fig. 4 Six types of three-phase transformer connection scheme

Topology reconfiguration in DNs is based on the switching scheme, the loads transfer between feeders can balance them and reduce the line loss. For annual simulation, the entire year is divided into 16 scenarios as shown in Table 2.

Table 2 Operating scenarios

Scenario			
1			
2	Spring (Mar, Apr, May)	Weekday	Day
3			Night
4	Weekend	Day	
5		Night	
6	Summer (Jun, Jul, Aug)	Weekday	Day
7			Night
8	Weekend	Day	
9		Night	
10	Fall (Sep, Oct, Nov)	Weekday	Day
11			Night
12	Weekend	Day	
13		Night	
14	Winter (Dec, Jan, Feb)	Weekday	Day
15			Night
16	Weekend	Day	
		Night	

In Table 2, the year is divided into four seasons: spring, summer, fall, and winter; each season is represented by two day types: weekday and weekend day; each of these days is divided into two periods: day and night. Therefore, the entire year is represented by 16 different operating scenarios (4 seasons/years×2 days/season×2 periods/day).

The topology reconfiguration scheme is based on these scenario to reach the optimal operating planning.

3.2 Multi-objective Programming

Three-phase unbalance is one of the main problem in DNs, it cause the increasing line loss, reverse torque of motor, and the malfunction of LCO relay in severe case. As far as system operation is concern, the system loss, voltage profile, neutral current, and load balancing between feeders is the most important for improving the power quality. These problems are the optimization objectives in this study, which is line loss, voltage profile, and neutral current in feeder outlet, respectively. Especially, neutral current in feeder circuit breaker (FCB) may give rise to malfunction of LCO protective relay in the three-phase, four-wire DNs, as shown in Fig. 5. The current of LCO is formulated as the three-phase current, which is equal to the neutral current. In Taipower, the LCO relay tripping setting limit value is around 70 A, and the LCO detects the neutral current over 70 A to trip the unbalanced short-circuit fault. Unfortunately, the high neutral current, which is caused by unbalanced loading and exceeds the limit value, can also lead to LCO tripping.

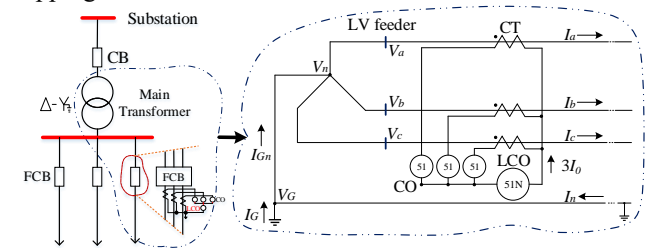


Fig. 5 The single line diagram of LCO protective relay in three-phase four-wire distribution systems.

Above-mentioned problems must be optimized simultaneously by algorithm, involving more than one objective function to be minimized or maximized is termed multi-objective optimization problem (MOOP). The methods to make trade-off between a set of feasible solution is proposed in many literatures. Assume for minimizing a bi-objective function (f_1, f_2), the feasible solution space in the coordinate plane is shown as Fig. 6. The points marked by blue circle dominates the yellow one because blue one is no worse than yellow one in all objectives. The non-dominated solutions which are not dominated by any member of the solution set is called the Pareto-optimal front (POF). Point C is not on the POF because it is dominated by both point A and point B, the points on POF is the set of best solution of the MOOP.

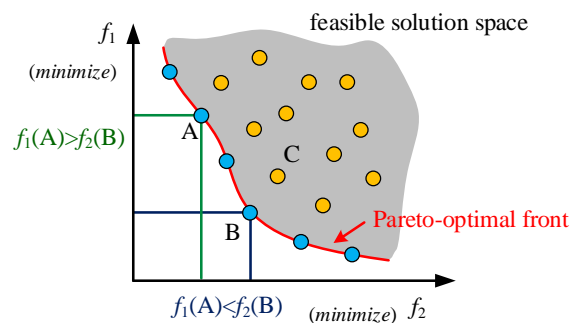


Fig. 6 Illustration of feasible solution and POF

To approximate the POF, weighted metric method, proposed by Zeleny in 1976 [11], Combine multiple objectives using the weighted distance metric of any solution from the ideal solution z^* , described as

$$\text{minimize } \left(\sum_{m=1}^M w_m |f_m(x) - z_i^*|^p \right)^{\frac{1}{p}} \quad (1)$$

$$\text{subject to } \sum_{m=1}^M w_m = 1$$

where integer $p=1,2,\dots,\infty$. Fig. 7 illustrates the weighted metric method. When $p=1$ it is similar to the weighted sum method by setting the z^* to $(0, 0)$, as shown in Fig. 7 (a); when $p=2$, it can be regarded as the weighted distance between the solution and z^* on plane coordinate, as shown in Fig. 7 (b); when $p \rightarrow \infty$, it can approximate all Pareto-optimal solutions, which is also called the weighted Tchebycheff metric, as shown in Fig. 7 (c). In this paper, the weighted Tchebycheff metric is used to combine the total line loss, voltage, and neutral line current in feeder outlet, and approximate the POF of feasible solution.

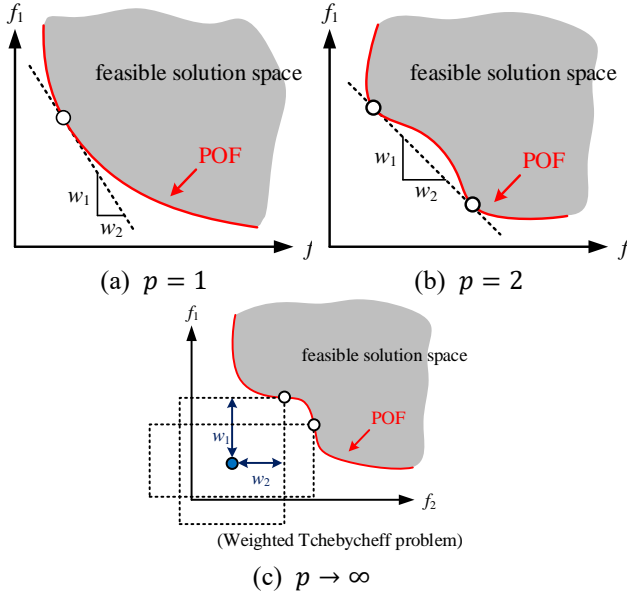


Fig. 7 Illustration of the weighted metric method

3.3 Constraints from Radial Topology

In this paper, the network topology must be kept radial. Therefore, there is a challenge during the switching scheme optimization because the switches operate randomly. To solve this problem, all the possible radial topologies should be identified, and only these topologies are worthy to calculate in optimization algorithm. In reference [12], the author proposed a procedure to identify all the possible radial configuration extracted from the weakly meshed structures of DNs based on the following steps:

Step 1) Create a reduced network structure which retains the same number of branches installed switches of the original network.

Step 2) Apply the reduced network of a simple computational procedure which called backtracking-based algorithm by graph theory described in [13] for identifying the radial structures.

Fig. 8 shows the reduced topology of sample system, it contain 11 TSs (T1-T11), 19 switches (B1~B9), and 21 reduced buses. Notably, the bus 1 present both S/S-1 and S/S-2 because they are regarded as one substation to prevent the connection between them. Afterwards, the backtracking-based computational procedure, which scans from source to end of network to check if it is radial configuration, is conducted to find all the possible radial topologies for each scenario. However, possible topologies is excessive, most of them are operationally improper, so it is not necessary to consider all of them in algorithm. To find the feasible radial topologies, the power flow snapshot of original and all the possible radial topologies are solved by distribution system simulator OpenDSS, and the topologies whose system loss are lower than original topology are chosen as the feasible topologies. These feasible switches state are saved to a database and extracted during the algorithm.

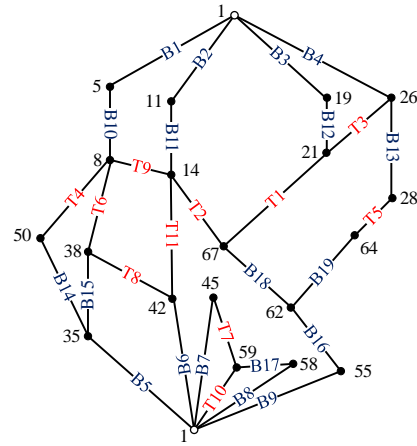


Fig. 8 Reduced topology of the sample system

3.4 Particle Swarm Optimization Algorithm

The particle swarm optimization (PSO) algorithm, proposed by Kennedy and Eberhart in 1995 [14], is a computational method that optimizes a problem by iteratively updating and improving the candidate solution. This algorithm is inspired by the flocks of spicity bird migration and forage behavior, two fundamental behaviors of which is concluded to cognition-only model and social-only model by observation. In a particle swarm, every particle represents a potential solution, and each of them owns its position and velocity. The movement of each particle is updated by three velocity component which are inertia (current motion influence), particle experience best (particle memory influence), and group experience best (swarm memory influence), as described in (2) and Fig. 9.

$$v_n^{i+1} = \omega v_n^i + \varphi_p \text{rand}() (p_{bestn}^i - s_n^i) + \varphi_g \text{rand}() (g_{bestn}^i - s_n^i) \quad (2)$$

$$s_n^{i+1} = s_n^i + v_n^{i+1}$$

where v_n^i is the particle n movement velocity at the i moment; and s_n^i is the position of particle n at the i moment. The parameters ω , φ_p , and φ_g denote the learning factor of inertia, particle, and swarm influence respectively. $\text{rand}()$ refers to the random number between 0 and 1.

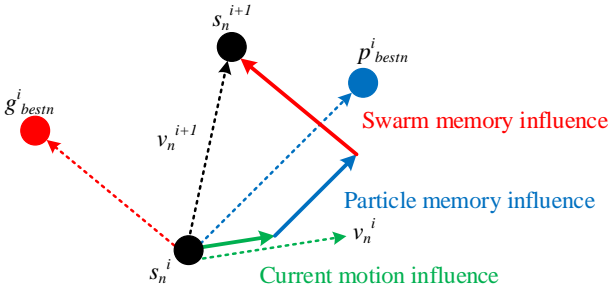


Fig. 9 Velocity component construction of PSO

The velocity of particle memory influence component is called the cognitive learning model; whereas the swarm influence one is referred to the social learning model. Thus, two models iterate and derive the optimal solution in the solution space. PSO is a metaheuristic as it makes few or no assumptions about the optimization problem and can search very large spaces of candidate solutions. However, metaheuristics such as PSO is unable to guarantee a global optimum must be found. In addition, PSO does not use the gradient of the problem, which means PSO is not necessary to make the optimization problem be differentiable which is required by other iterative optimization methods such as gradient descent. PSO is used to solve the MOOP in this paper, each particle represent all the switching scheme and connection scheme of transformers.

IV. Implementation of Proposed Platform

4.1 Overall Architecture of Proposed Platform

The architecture of proposed platform is shown in Fig. 10, and can be divided into main block and data exchange block. Initially, the circuit model in OpenDSS and PSO algorithm parameters setup are executed in main block, then PSO randomly generate particle position and velocity and input to data exchange block. The particles position are converted to switch states and transformer connections, and python give switching and rephase commands to OpenDSS via COM. Next, OpenDSS solves circuit and returns annual power flow to python. The PSO algorithm update particle velocity and position base on the power flow over and over again, finally it stop searches when the maximum number of iteration is reached and export and plot the optimal result. Notably, the switches state is derived from a database which collects the switches state of feasible radial topologies for each scenario.

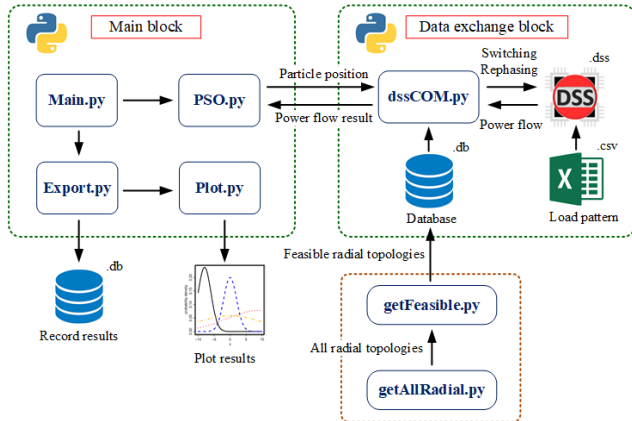


Fig. 10 Architecture of proposed platform

4.2 Optimization Result and Discussion

Table 3 shows the PSO algorithm parameters of four test cases. The objective function of the MOOP in this paper (weighted Tchebycheff metric) is described as

$$OF = \left[\omega_1 \left(\frac{E_{loss}^i - E_{loss}^{min}}{E_{loss}^{max} - E_{loss}^{min}} \right)^p + \omega_2 \left(\frac{\Delta V^i - \Delta V^{min}}{\Delta V^{max} - \Delta V^{min}} \right)^p + \omega_3 \left(\frac{I_n^i - I_n^{min}}{I_n^{max} - I_n^{min}} \right)^p \right]^{\frac{1}{p}} \quad (3)$$

where E_{loss}^i is the total energy loss (kWh); ΔV^i is the average bus voltage drop (p.u.); I_n^i is the maximum neutral current in FCBs (A). ω_1, ω_2 , and ω_3 are the weights of them respectively. p is set to 100 to approximate the non-convex POF. Moreover, a normalization process compresses each of objective into unit because of their different scales. Case 1~3 only set one weight to 1 to optimize one objective individually; case 4 average three weights to optimize all the objectives. The optimal solution of all cases compared are shown in

Table 4, Fig. 11 shows the iterative convergence process of objective function.

Table 3 PSO parameters of four test cases

Case	Parameters							
	Swarm size	Iterations	ω	φ_p	φ_g	ω_1	ω_2	ω_3
Case 1			from			1	0	0
Case 2	100	100	0.9 to 0.4	0.5	0.5	0	1	0
Case 3			during			0	0	1
Case 4			iteration			0.4	0.3	0.3

Table 4 Performance comparison of four cases

Case	Result			
	Object function	E_{loss} (kWh)	ΔV (p.u.)	I_n (A)
Original	-	312.5136	0.0161	28.61
Case 1	0.8735	272.9865	0.0155	27.32
Case 2	0.9509	286.7001	0.0153	38.54
Case 3	0.6322	288.2820	0.0161	18.09
Case 4	0.3520	275.0345	0.0155	22.98

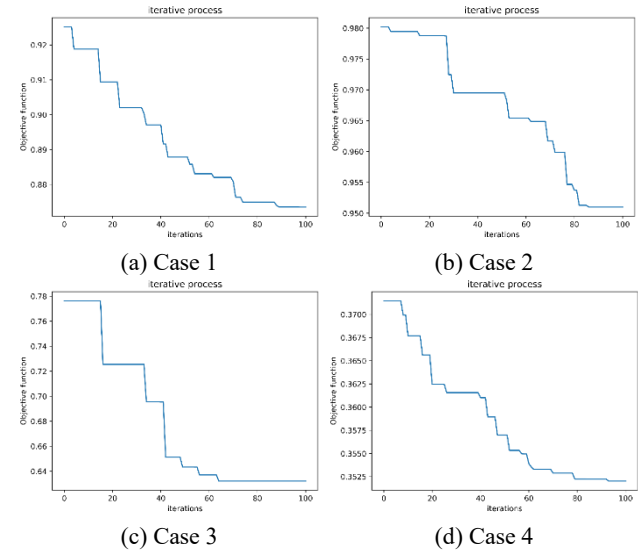


Fig. 11 Iterative process of objective function for each case
Fig. 12 shows the feeder total energy loss for each case. Although the loss in feeder F1 and F2 increase in some cases, the loss in feeder F4 decrease dramatically, the total loss is hence reduced. The total loss is reduced by about 12.65 % in case1 and 11.99 % in case 4, but even so, the result of case 4 is preferred because the neutral current in FCB can also be reduce to prevent the malfunction of LCO.

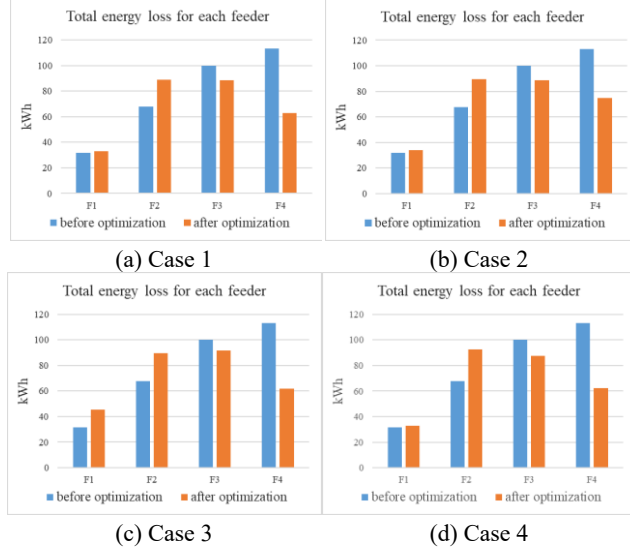


Fig. 12 Improvement of feeder total energy loss for each case

Fig. 13 show the improvement of neutral current on FCBs for case 3. It is distinct that the neutral current has different average values for each season, because the connection of transformers are rearranged seasonally. The maximum neutral current in FCBs is reduced to 18.09 A in case 3. The result of case 4 is preferred due to the higher reduction of total energy loss.

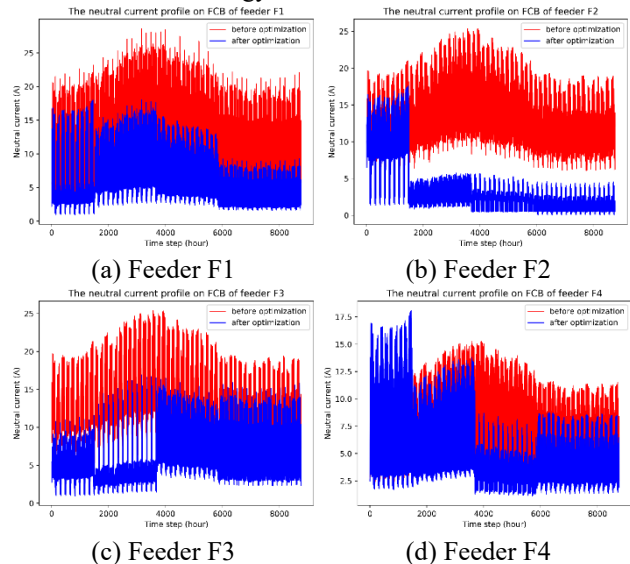


Fig. 13 Improvement of neutral current on FCBs for case 3

V. Conclusion

In this paper, an integrated dynamic topology reconfiguration and phase arrangement optimization simulation platform is proposed. Both of them are optimized simultaneously while keeping the topology radial configuration. The results show that the total energy

loss is reduced because of the load balancing between feeders, and the maximum neutral current on FCBs is reduced due to the phase balancing. The outcomes of this research are helpful for system operator; moreover, the proposed systematic calculation and the comprehensive optimization scheme can reduce operation cost, improve the system stability and power quality efficiently.

Acknowledgment

本研究承蒙核能研究所計畫編號：109A010 之經費補助研究計畫之經費補助，特此感謝。

Reference

- [1] H. Sekhavatmanesh, and R. Cherkaoui, "Optimal Infrastructure Planning of Active Distribution Networks Complying With Service Restoration Requirements" *IEEE Transactions on Smart Grid*, Vol. 9, No. 6, pp. 6566-6577, 2018.
- [2] S.-B. Lei, Y.-H. Hou, F. Qiu, and J. Yan, "Identification of Critical Switches for Integrating Renewable Distributed Generation by Dynamic Network Reconfiguration" *IEEE Transactions on Sustainable Energy*, Vol. 9, No. 1, pp. 420-432, 2018.
- [3] Z.-F. Tan, H.-W. Zhong, J.-X. Wang, et al., "Enforcing Intra-Regional Constraints in Tie-Line Scheduling: A Projection-Based Framework" *IEEE Transactions on Power Systems*, Vol. 34, No. 6, pp. 4751-4761, 2019.
- [4] Z.-G. Li, M. Shahidepour, W.-C. Wu, et al., "Decentralized Multiarea Robust Generation Unit and Tie-Line Scheduling Under Wind Power Uncertainty" *IEEE Transactions on Sustainable Energy*, Vol. 6, No. 4, pp. 1377-1388, 2015.
- [5] A. Ameli, A. Ahmadifar, M.-H. Shariatkah, et al., "A Dynamic Method for Feeder Reconfiguration and Capacitor Switching in Smart Distribution Systems" *International Journal of Electrical Power & Energy Systems*, Vol. 85, pp. 200-211, 2017.
- [6] M. J. E. Alam, K. M. Muttaqi, and D. Sutanto, "Community Energy Storage for Neutral Voltage Rise Mitigation in Four-Wire Multigrounded LV Feeders With Unbalanced Solar PV Allocation" *IEEE Transactions On Smart Grid*, Vol. 6, No. 6, pp. 2845-2855, 2015.
- [7] Y.-D. Lee, J.-L. Jiang, Y.-H. Ho, et al., "Neutral Current Reduction in Three-Phase Four-Wire Distribution Feeders by Optimal Phase Arrangement Based on a Full-Scale Net Load Model Derived from the FTU Data" *Energies*, Vol. 13, No. 7, pp. 1844, 2020.
- [8] M.-Y. Huang, C.-S. Chen, C.-H. Lin, et al., "Three-phase balancing of distribution feeders using immune algorithm" *IET Generation, Transmission & Distribution*, Vol. 2, No. 3, pp. 383-392, 2008.
- [9] C.-H. Lin, C.-S. Chen, H.-J. Chuang, et al., "An Expert System for Three-Phase Balancing of Distribution Feeders" *IEEE Transactions on Power Systems*, Vol. 23, No. 3, pp. 1488-1496, 2008.
- [10] D. Das, "A fuzzy multiobjective approach for network reconfiguration of distribution systems" *IEEE Transactions on Power Delivery*, Vol. 21, No. 1, pp. 202-209, 2006.
- [11] Milan Zeleny, "The Attribute-Dynamic Attitude Model (Adam)" *Management Science*, Vol. 23, No. 1, 1976.
- [12] H. Andrei, and G. Chicco, "Identification of the Radial Configurations Extracted From the Weakly Meshed Structures of Electrical Distribution Systems" *IEEE Transactions on Circuits and Systems*, Vol. 55, No. 4, pp. 1149-1158, 2008.
- [13] H. Andrei, I. Caciula, and G. Chicco, "An efficient algorithm for forming radial structures from weakly meshed networks" *Proc. VI World Energy Syst. Conf.*, Torino, Italy, Jul. 10-12, 2006, pp. 175-180.
- [14] J. Kennedy and R. Eberhart, "Particle swarm optimization" *Proceedings of ICNN'95 - International Conference on Neural Networks*, pp. 1942-1948, 1995.